

# 黔西北大方地区龙潭组海陆过渡相烃源岩特征及评价

兰叶芳,任传建,潘仕辉,任戍明

(贵州工程应用技术学院 矿业工程学院, 贵州 毕节 551700)

**摘要:** 黔西北大方地区龙潭组以泥页岩、煤层与砂岩交替互层发育为特点,具有典型的海陆过渡相特征。文章在剖面实测和样品采集的基础上,结合全岩和黏土矿物XRD分析、总有机碳(TOC)含量测定、岩石热解、干酪根显微组分及镜质体反射率( $R_o$ )等分析,对研究区龙潭组烃源岩发育特征进行了研究和评价。结果表明:①龙潭组矿物以黏土矿物为主,具有较强的吸附能力,但黏土矿物含量与石英含量呈明显的负相关关系( $R>0.8$ ),尤其是泥页岩中70%以上的黏土含量以及较低的脆性指数增加了压裂开发的难度。②龙潭组有机质丰度受岩性变化控制明显。煤层具有最高的TOC含量(平均值42.9%)和生烃潜量(平均值为2.68 mg/g),显示强大的煤层气生烃潜力;泥页岩生烃潜量均小于2 mg/g,但约有80%样品的TOC含量超过2%,页岩气资源潜力不及煤层气;粉砂岩生烃潜力最差,生烃潜量平均值为0.13 mg/g,TOC含量为1.4%~5.6%,显示一定的致密气潜力。③龙潭组有机显微组以壳质组和镜质组占主导,干酪根以Ⅲ型为主,Ⅱ<sub>2</sub>型为辅,热演化程度高,处于高-过成熟的生气阶段。④煤层更为发育的龙潭组中段是大方地区煤层气、页岩气和致密砂岩气联合勘探的有利时段。

**关键词:** 海陆过渡相; 龙潭组; 非常规气; 烃源岩; 黔西北

中图分类号: P588.2; P618.13

文献标识码: A

文章编号: 1000-6524(2023)06-0852-16

## Characteristics and evaluation of marine-terrestrial transitional source rocks in the Longtan Formation in the Dafang area, Northwest Guizhou

LAN Ye-fang, REN Chuan-jian, PAN Shi-hui and REN Shu-ming

(School of Mining Engineering, Guizhou University of Engineering Science, Bijie 551700, China)

**Abstract:** The Longtan Formation in the Dafang area of Northwest Guizhou is characterized by alternated shale, coal seams, and sandstones, with typical characteristics of marine-terrestrial transitional facies. On the basis of profile measurement and sample collection, combined with XRD analysis of whole rock and clay minerals, determination of total organic carbon (TOC) measurement, rock pyrolysis, kerogen macerals, and vitrinite reflectance ( $R_o$ ) analysis, the development characteristics of hydrocarbon source rocks of the Longtan Formation in the study area are studied and evaluated. The results indicate that: ① The minerals in the rocks of the Longtan Formation are mainly clay minerals with strong adsorption capacity, but there is a significant negative correlation between clay mineral content and quartz content ( $R>0.8$ ), especially the clay content of over 70% in shale and the lower brittleness index, which is very unfavorable for fracturing development; ② The abundance of organic matter in the Longtan Formation is significantly controlled by lithology. The coal seam has the highest TOC content (average 42.9%) and hydrocarbon

收稿日期: 2023-06-09; 接受日期: 2023-08-01; 编辑: 曲丽莉

基金项目: 贵州省科技计划项目(黔科合基础[2017]1407); 高层次人才科研启动基金项目(院科合字G2017006号); 贵州省青年科技人才成长项目(黔教合KY字[2016]283); 创新创业项目(S202210668115)

作者简介: 兰叶芳(1984- ), 女, 博士, 副教授, 主要从事沉积地质学领域的教学和科研工作, E-mail: wssbdnn@163.com。

generation potential (average 2.68 mg/g), indicating strong hydrocarbon generation potential of coalbed methane; The hydrocarbon generation potential of shale is less than 2 mg/g, but about 80% of the samples have TOC content exceeding 2%, and the shale gas resource potential is less than that of coalbed methane; Silty sandstone has the worst hydrocarbon generation potential, with an average hydrocarbon generation potential of 0.13 mg/g and a TOC content of 1.4%~5.6%, indicating a certain degree of tight gas potential; ③ The macerals of the Longtan Formation kerogen are mainly composed of liptinite and vitrinite, with type III kerogen being the main type and type II<sub>2</sub> being the auxiliary type. They have a high degree of thermal evolution and are in the stage of high-over mature dry-gas generation; ④ The middle section of the Longtan Formation, where coal seams are more developed, is a favorable zone for joint exploration of coalbed methane, shale gas, and tight sandstone gas in the Dafang area.

**Key words:** marine-terrestrial transitional facies; Longtan Formation; unconventional natural gas; source rock; Northwest Guizhou

**Fund support:** Guizhou Science and Technology Program Project (Qiankehe Foundation [2017]1407); High-level Talent Research Startup Fund Project (G2017006); Guizhou Province Youth Science and Technology Talent Growth Project (Qianjiaohe KY[2016] 283); Innovation and Entrepreneurship Project (S202210668115)

我国海陆过渡相页岩气资源丰富,约占页岩气总资源量的1/4(匡立春等,2020)。二叠系海陆过渡相富有机质泥页岩层系分布广泛,主要有以山西组、太原组和龙潭组为代表的含煤建造型和以孤峰组、大隆组为代表的含硅质建造型(翟刚毅等,2020;曹磊等,2020)。相较于目前已达到商业化开发阶段的海相页岩气研究而言,海陆过渡相页岩气的整体研究与勘探开发程度较低(邓敏等,2022),陆相页岩油和海陆过渡相页岩气处于工业探索阶段(邹才能等,2020),海陆过渡相与陆相页岩气的突破和工业化生产是实现中国页岩气规模化发展的重要环节(董大忠等,2016)。近年来,海陆过渡相油气勘探引起了中石化、中石油等企业以及相关科研院所和生产单位的重视,陆续在鄂尔多斯盆地、四川盆地及其周缘、南华北盆地、柴达木盆地以及下扬子地区布设以海陆过渡相为目的层的非常规油气探井(郭旭升等,2018;李剑等,2021;董大忠等,2021),尤其在四川盆地、鄂尔多斯盆地等海相页岩气研究比较深入的地区,海陆过渡相页岩气勘探展现出良好前景(张金川等,2021;焦方正等,2023),如鄂尔多斯盆地针对海陆过渡相页岩实施的吉平1H井目前日产气量稳定在 $3.50 \times 10^4 \text{ m}^3$ (郭为等,2023),以及最近中石化在四川盆地东南部重庆南川地区部署了风险探井——YY1井,压裂试气获得二叠系龙潭组阶段页岩气产量约 $4\,000 \text{ m}^3/\text{d}$ (何贵松等,2023)。

贵州属于多煤、少气、贫油的省份,但具有非常规气良好的成矿条件和找矿潜力。数据显示,贵州页岩气数据地质资源量达13.54万亿立方米,排名

位居全国第3位(孙文吉斌,2021),凸显了贵州巨大的页岩气勘探潜力。在黔北金沙复杂构造区已获得二叠系龙潭组页岩气、煤层气和致密砂岩气协同发现(王胜建等,2020),而西页1井、东神页1井、方页1井及金沙页1等井龙潭组现场解析具有 $0.6 \sim 19.2 \text{ m}^3/\text{t}$ 不等的含气量(张金川等,2021)。页岩气、煤层气和致密砂岩气资源将成为未来贵州省天然气供给的重要补充。然而,与传统天然气勘探开发相比,非常规天然气具较强特殊性(聂海宽等,2011;胡海洋等,2019),尤其在有机质类型特点及其生气条件评价、压力系统研究等方面与以往工作思路和方法存在较大差异。虽然在海陆过渡相地层中发现了少量获得工业规模气流的生产井,但整体效果不是特别理想,距离建成商业化气田还有较远距离(魏晓亮,2020),需要进一步针对海陆过渡相非常规气生烃潜力与资源评价方法、赋存机理与主控因素、储集空间的构成及演化、微孔结构及物性条件、甜点区/段识别和预测等不断试验和探索。该研究选取黔西北大方地区龙潭组海陆过渡相地层为研究对象,结合野外地质工作和实验分析结果,探索黔西北海陆交互相龙潭组非常规气烃源岩特征、发育地质条件与勘探潜力,以期为黔西北地区非常规气的勘探开发提供一定的参考。

## 1 区域地质背景

大方地区位于贵州西北部,构造上属于黔中隆起(图1a),区内褶皱和断层发育(李娟等,2015)。震

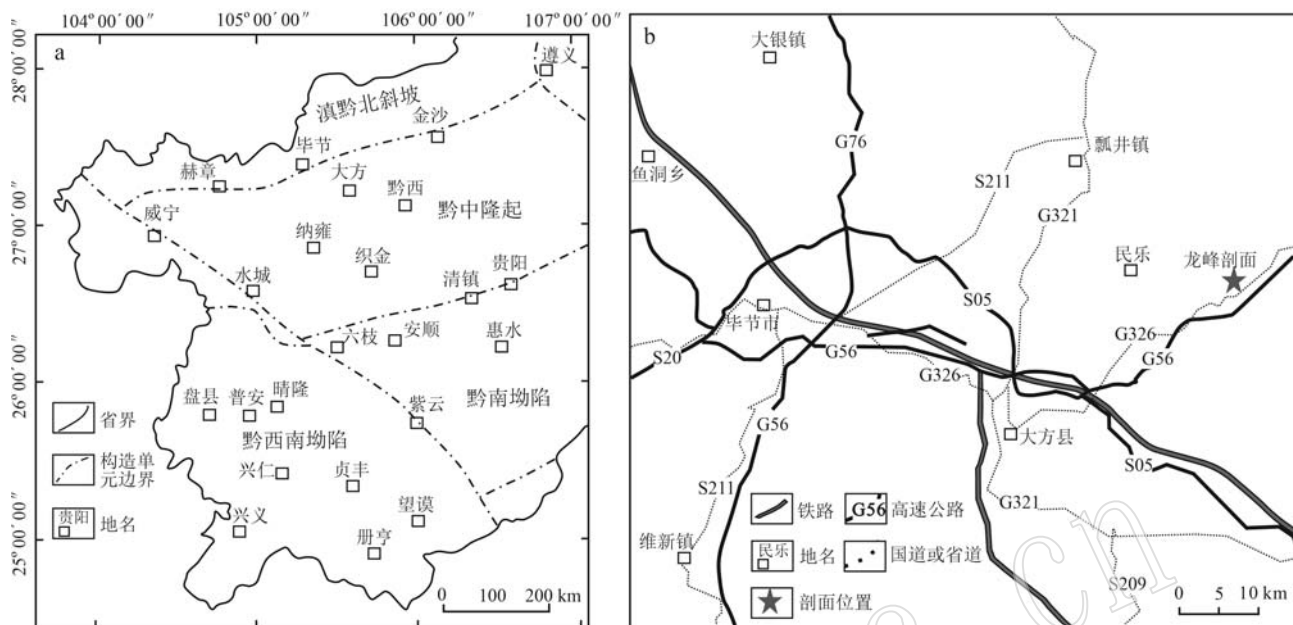


图1 黔西北及其邻区构造分区图[a, 据马啸(2021)修改]和采样剖面位置图(b)

Fig. 1 Structural map of Northwest Guizhou and its adjacent areas (a, modified from Ma Xiao, 2021) and the location of sampling profile (b)

旦纪至中三叠世期间,该区没有明显的造山运动,仅有海水升降运动,基本处于广海台地和潮坪环境。早寒武世龙王庙期开始受加里东运动影响,黔中地区海水逐渐退出,台地大面积露出水面,隆升为陆,黔中隆起形成。随着隆起范围逐渐向北和向西扩大,与川南古陆联成一片,直至早二叠世初海水大范围扩大覆盖研究区(孙全宏, 2014)。晚奥陶世至二叠纪,加里东运动抬升贵州中部。当时受长期风化剥蚀作用,导致该地大部分地区不发育下二叠统。晚二叠世东吴运动期间,贵州西北部发生了广泛的海退作用。由于北东向海水的退缩,该地区沉积环境由陆表海变为海陆过渡相沉积(图2)。在此阶段,海陆过渡相龙潭组碎屑岩在该区广泛沉积。龙潭组沉积之后,主要遭受了海西晚期运动、安源运动、燕山运动以及喜马拉雅运动的破坏和影响,背斜多被伴生断层破坏,保存较好的龙潭组大多发育于开阔的向斜或者部分背斜核部(刘曾勤, 2020),其中研究区所处的大方背斜总体为北北东向褶皱(贾立龙等, 2021),实测剖面位置如图1b所示。

## 2 野外剖面、样品采集与测试

大方地区龙潭组在地表出露广泛,地层厚度大致变化在110~195 m之间,主要沿大方背斜翼部呈

带状分布,为一套由砂岩、粉砂岩、黏土岩夹煤层及少量灰岩等组成的地层,常含植物化石,可见腕足、双壳等动物化石发育的海陆交互相沉积组合。区内该套地层下伏与茅口组碳酸盐岩平行不整合接触,上覆与长兴组灰岩地层整合接触。此次研究选择较为典型的百纳乡龙峰剖面进行详细实测和采样(图3)。该剖面龙潭组的顶底地层界限清晰(图4a、4b),易于识别,基岩出露大约95%,沿公路进行剖面实测,测制条件也比较优越。

此次共采集露头样品44件。经过实验前样品预处理之后,样品在中国石油勘探开发研究院实验中心进行全岩和黏土矿物X射线衍射分析(XRD)、总有机碳(TOC)测定、岩石热解(Rock-Eval)、干酪根显微组分及镜质体反射率( $R_o$ )分析。

## 3 岩石学与矿物学特征

### 3.1 岩石学特征

大方地区龙峰剖面龙潭组下段厚约23.9 m,以深灰色-灰黑色薄层泥岩为主,底部为浅灰色凝灰质或铝土质泥岩,顶部多为含植物根茎化石的浅灰色薄层泥岩,上部发育真厚度约2.5 m的煤层。龙潭组中段厚约67.7 m,以细砂岩、粉砂岩发育(夹泥页

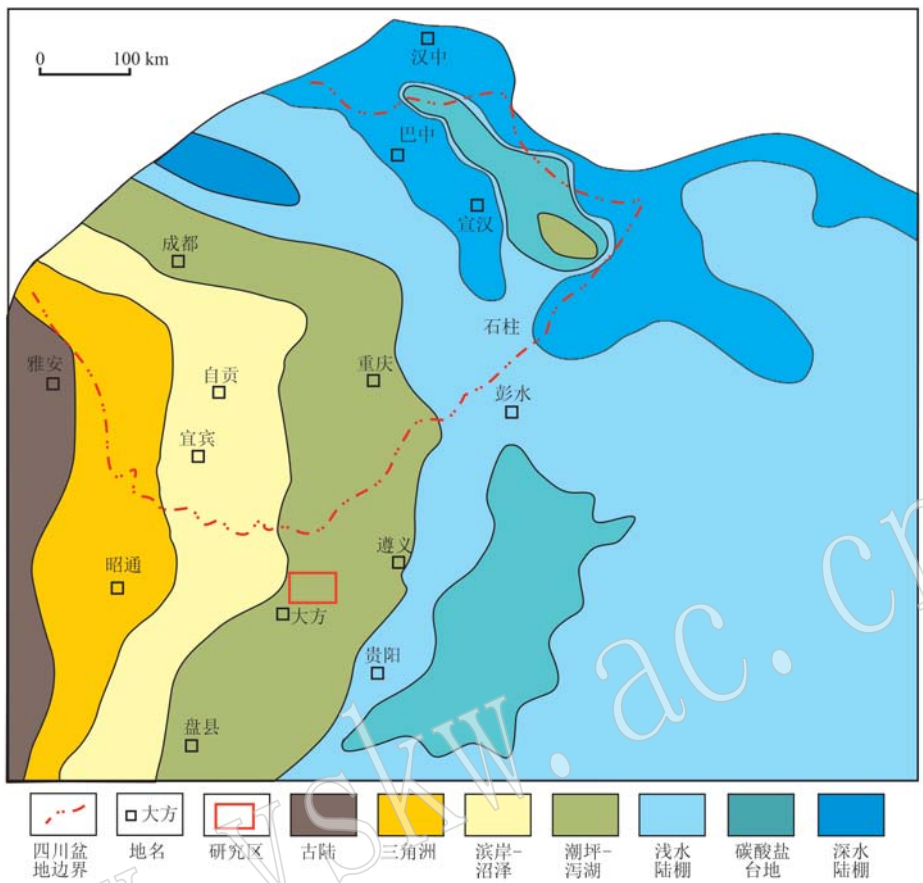


图2 黔西北及其周缘上二叠统龙潭组沉积相图[据冯动军(2023)修绘]

Fig. 2 Sedimentary facies map of the Upper Permian Longtan Formation in Northwest Guizhou and its surrounding areas  
(modified from Feng Dongjun, 2023)

岩薄层)为标志与下段相区分,以薄层砂泥岩互层与煤层交替发育为主体特征,顶部多以优质煤层的结束以及泥页岩的发育作为与上段的界限,水平层理或页理发育,泥页岩与粉砂岩以及炭质页岩与泥岩之间多呈互层发育(图4c,4g),该段同时发育不同厚度的煤层,亦可见构造揉皱现象(图4f)。龙潭组上段厚约60.5 m,以粉砂岩的出现为始,普遍发育极薄层泥岩,中上部发育数层粉砂岩和灰岩夹层,以灰色、灰黑色薄-极薄层泥岩为主,地层中粉砂岩(泥质粉砂岩)与泥岩(页岩)组成的韵律层理常见,泥岩中水平层理普遍发育(图4h,4i),同时可见灰岩呈透镜体分布在泥岩中,构成透镜状层理。

此外,煤层主要发育在龙潭组中下段地层中(上段仅见极薄层的劣煤),煤层与煤线中常见立方体状黄铁矿发育。褐黄色泥岩、灰白色泥岩与灰色、灰黑色泥岩中发育大量植物根茎化石以及 *Gigantonoclea largelii*(波缘单网羊齿)、*Rhipidopsis panii*(楔扇叶)等植物叶片,其形态和轮廓均保存较为完好(图

4d,4e)。

根据薄片分析结果,龙潭组的下伏地层茅口组发育泥晶-亮晶生屑灰岩,生屑以有孔虫为主,见棘皮动物发育(图5a)。龙潭组的上覆地层长兴组发育泥晶生屑灰岩,生屑以有孔虫为主(图5b)。龙潭组下段主要发育炭质泥页岩(有时含少量粉砂)以及煤层,顶部为薄层砂岩,该段岩石网状微裂缝发育(图5c);龙潭组中段主要为泥(页)岩与粉砂岩的交替发育(图5d~5i),泥页岩和煤层中植物化石常见;龙潭组上段以发育碳质(泥质)粉砂岩、(铁质)粉砂质-碳质泥岩、泥质粉砂岩、泥岩(微裂缝发育)为主(图5j~5l),含生物化石碎片,发育微裂缝,微裂缝中充填亮晶方解石,顶部发育富含黄铁矿的生屑灰岩以及亮晶-泥晶生屑灰岩,生屑包括腕足、有孔虫、棘皮类动物等,生屑灰岩中往往发生选择性白云化作用(图5m~5p)。

### 3.2 矿物学特征

岩石矿物组成是页岩气开发的重要组成部分,

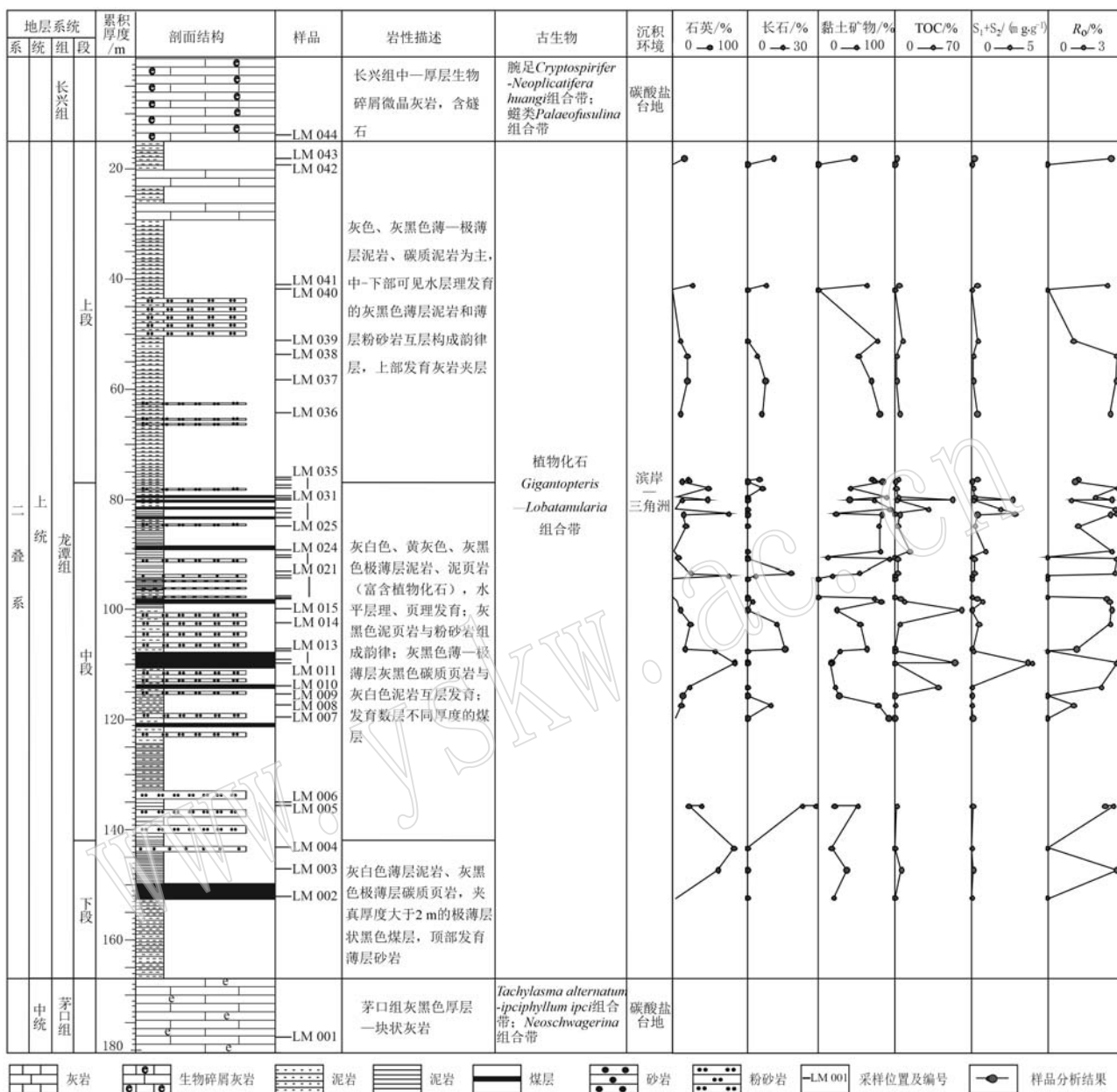


图3 黔西北大方地区龙峰剖面龙潭组地层综合柱状图

Fig. 3 Stratigraphic column of Longtan Formation in Longfeng profile of Dafang area, Northwest Guizhou

特别是对于页岩的有利压裂目标层而言,有机质(含量大于3%)和脆性矿物(含量大于50%)为裂缝的发育提供了重要的物质基础(袁余洋等,2020)。全岩及黏土矿物X射线衍射分析表明,大方地区龙峰剖面龙潭组岩石中黏土矿物是最主要的组分(图6、图7),其含量为31%~77%,平均58.7%,以伊/蒙混层和伊利石为主(约占黏土矿物总量的85%),其余绿泥石和高岭石在黏土矿物中的占比分别大约为11.7%和3.6%(图6b)。伊/蒙混层矿物含量较高,

反映当时的沉积环境为贫氧的相对还原的环境,有利于有机质的保存与富集,给烃类气体的生成与富集提供了良好的环境(邓恩德等,2020a)。其次是石英,含量为8%~62%,平均25.5%,粉砂岩中石英含量为13.0%~82.1%,泥(页)岩中则为2.7%~25.9%(图6a),这与黔西、黔西北以及四川盆地龙潭组的矿物组成总体趋势一致(李娟等,2015; 邓恩德等,2020a; 王晓蕾等,2020; 邓敏等,2022)。龙潭组地层中长石以斜长石为主,钾长石少见,长石在岩

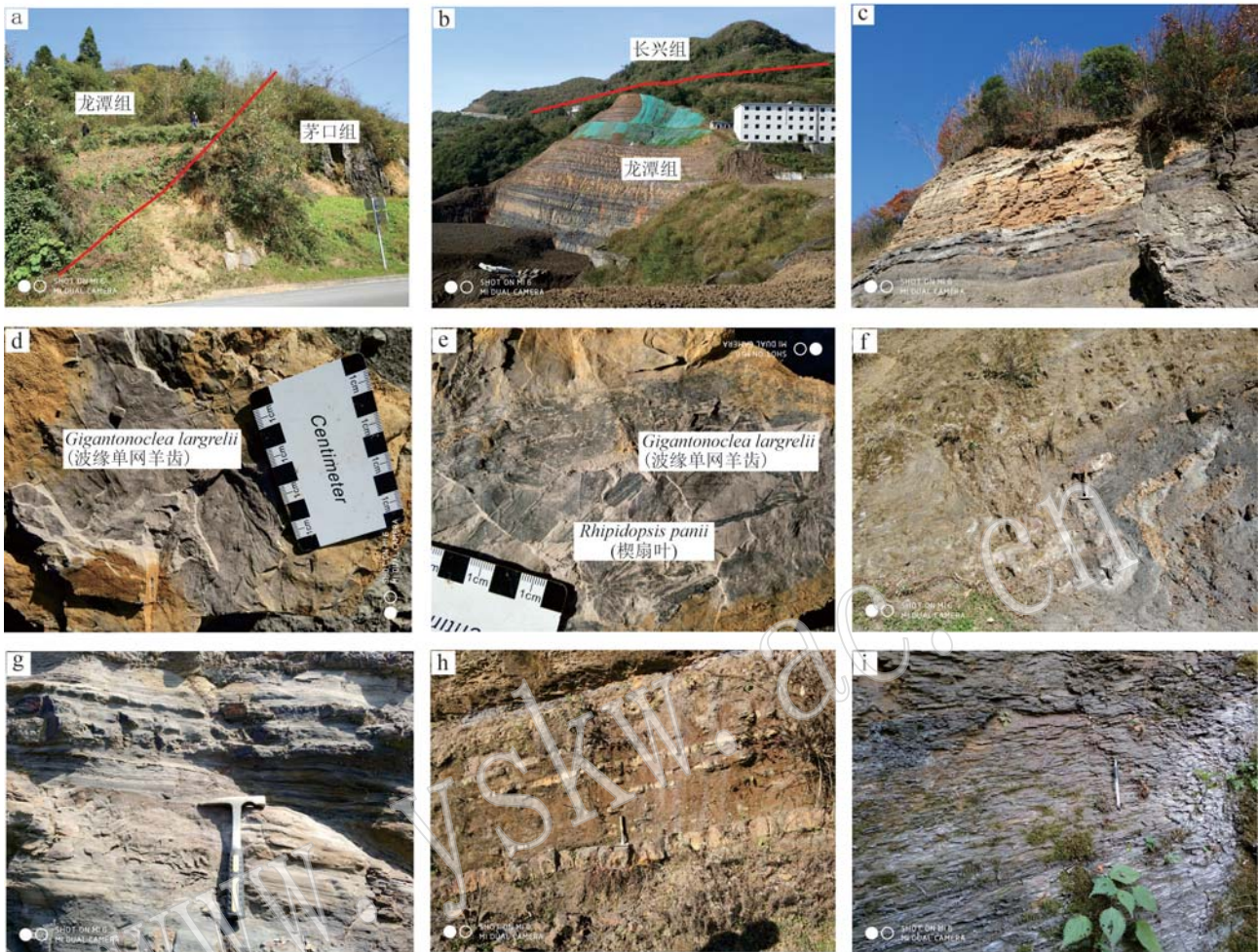


图4 黔西北大方地区龙峰剖面龙潭组野外宏观照片

Fig. 4 Field macroscopic photos of Longtan Formation in Longfeng profile of Dafang area, Northwest Guizhou

a—茅口组与龙潭组界线；b—龙潭组与长兴组界线，可见龙潭组地层中发育数层煤线/煤层；c—下部为灰黑色碳质泥岩与灰色泥岩组成的韵律层理，上部为土黄色泥岩与泥质粉砂岩组成的韵律层理；d—泥页岩中发育大量植物化石，以波缘单网羊齿(*Gigantonoclea largelii*)为主；e—轮廓较为清晰的波缘单网羊齿(*Gigantonoclea largelii*)和楔扇叶(*Rhipidopsis panii*)共同发育于泥页岩中；f—龙潭组地层中发育的小的揉皱(挠曲)；g—粉砂岩与泥岩互层发育，泥岩中发育水平层理；h—泥质粉砂岩与泥岩互层出现；i—龙潭组顶部发育的极薄层灰色泥页岩

a—the boundary between the Maokou Formation and the Longtan Formation; b—the boundary between the Longtan Formation and the Changxing Formation, showing several coal seams in the Longtan Formation; c—the lower part is a rhythmic bedding composed of gray black carbonaceous mudstone and gray mudstone, and the upper part is a rhythmic bedding composed of soil yellow mudstone and muddy siltstone; d—plant fossils (mainly *Gigantonoclea largelii*) are developed in the shale; e—the *Gigantonoclea largelii* and *Rhipidopsis panii* are developed in shales; f—small crumpling (bending) developed in the Longtan Formation; g—siltstone and mudstone are interbedded, and horizontal bedding is developed in mudstone; h—interbedded appearance of muddy siltstone and mudstone; i—the extremely thin layer of gray shale developed at the top of the Longtan Formation

石中的平均含量为4.6%，而碳酸盐矿物(方解石+铁白云石+菱铁矿)除在个别样品中含量较高外，总体不发育，在岩石中的平均含量为3.1%。锐钛矿虽然平均含量不高(其在岩石中的平均含量为2.6%)，但在龙潭组地层中普遍发育，含量大多在1%~5%之间。此外，样品中发育少量黄铁矿、针铁矿等其他矿物。

纵向上，自龙潭组下段至龙潭组上段，黏土矿物含量呈逐渐增加的趋势，而石英含量则逐渐降低(图6c)，并且从二者的相关图中可以看出，黏土矿物含量与石英含量呈明显的负相关关系，相关系数在0.8以上(图7b)，这表明在搬运过程中沉积物的数量和组成发生了显著变化，反映了过渡相沉积环境水体频繁动荡、沉积微相变迁较快、水动力强度变化较快

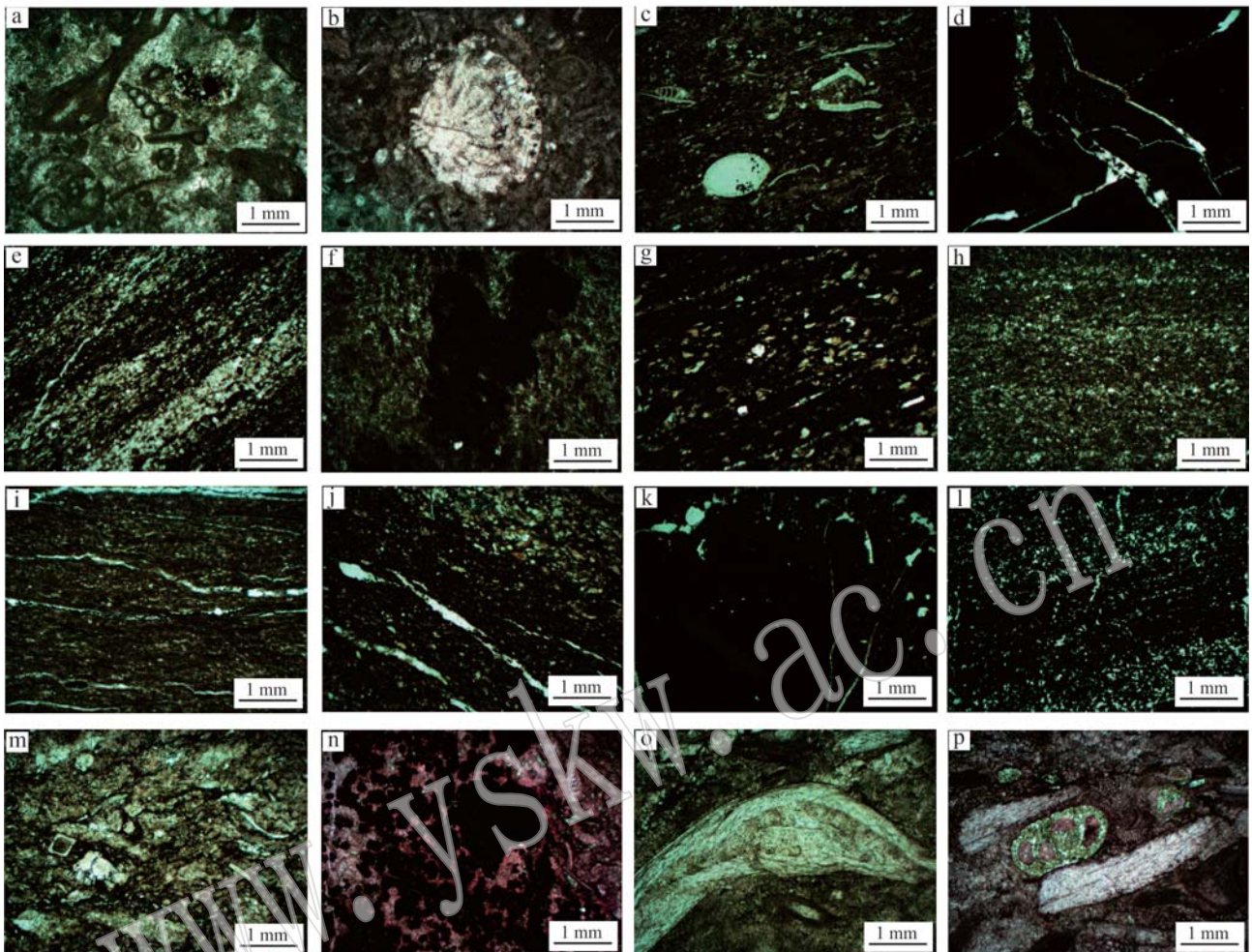


图 5 黔西北大方地区龙峰剖面龙潭组及上下地层岩石薄片显微特征

Fig. 5 Microscopic characteristics of the rocks from the Longtan Formation and its upper and lower strata in the Longfeng profile of the Dafang area, Northwest Guizhou

a—茅口组顶部发育的泥晶—亮晶生屑灰岩,生物碎屑以单列有孔虫、底栖有孔虫为主,可见少量棘皮动物发育,样品号 LM001,普通薄片,单偏光; b—长兴组底部发育的泥晶生屑灰岩,照片中心为有孔虫,样品号 LM044,普通薄片,茜素红 S 染色,单偏光; c—粉砂质泥岩,发育有孔虫、双壳、介形虫等生物碎屑,样品号 LM004,普通薄片,单偏光; d—煤岩中发育网状微裂缝,样品号 LM010,普通薄片,单偏光; e—泥质碳质粉砂岩,水平层理发育,富含有机质的暗色层和粉砂层交替出现,样品号 LM019,普通薄片,单偏光; f—铁质砂岩/粉砂岩,样品号 LM020,普通薄片,单偏光; g—粉砂质碳质泥页岩,有机质含量高,样品号 LM026,普通薄片,单偏光; h—泥质粉砂岩,样品号 LM032,普通薄片,单偏光; i—泥岩,微裂隙发育,样品号 LM035,普通薄片,单偏光; j—富有机质粉砂质泥岩,微裂隙发育,样品号 LM036,普通薄片,单偏光; k—煤岩中发育少量的石英粉砂,样品号 LM023,普通薄片,单偏光; l—煤岩中发育层状分布的粉砂级石英,样品号 LM030,普通薄片,单偏光; m—龙潭组顶部发育的生物碎屑灰岩,样品号 LM040,普通薄片,单偏光; n—生物碎屑灰岩中发育斑块状分布的黄铁矿,样品号 LM040,普通薄片,茜素红 S 染色,单偏光; o—泥晶生物碎屑灰岩,照片中心为腕足化石碎片,样品号 LM042,普通薄片,单偏光; p—泥晶生物碎屑灰岩,见腕足化石碎片以及发生选择性白云化作用的有孔虫,样品号 LM042,普通薄片,茜素红 S 染色,单偏光

a—the bioclastic limestone developed at the top of the Maokou Formation, with bioclastic mainly consisting of monoclinic foraminifera and benthic foraminifera, and small amount of echinoderms, LM001, ordinary thin section, single polarized light; b—the bioclastic limestone developed at the bottom of the Changxing Formation, with foraminifera in the center of the photo, LM044, ordinary thin section, stained with alizarin red S, single polarized light; c—silty mudstone with bioclasts such as foraminifera, bivalves, and ostracods, LM004, ordinary thin section, single polarized light; d—reticulate microcracks developed in the coal rocks, LM010, ordinary thin section, single polarized light; e—argillaceous and carbonaceous siltstone with horizontal bedding, alternating dark and silty layers rich in organic matter, LM019, ordinary thin section, single polarized light; f—iron sandstone/siltstone, LM020, ordinary thin section, single polarized light; g—silky carbonaceous shale with high organic matter content, LM026, ordinary thin section, single polarized light; h—argillaceous siltstone, LM032, ordinary thin section, single polarized light; i—mudstone with microcracks, LM035, ordinary thin section, single polarized light; j—silky mudstone rich in organic matters and microcracks, LM036, ordinary thin section, single polarized light; k—a small amount of quartz developed in the coal rock, LM023, ordinary thin section, single polarized light; l—stratified distribution of silt grade quartz is developed in the coal rock, LM030, ordinary thin section, single polarized light; m—the bioclastic limestone developed at the top of the Longtan Formation, LM040, ordinary thin section, single polarized light; n—patchy pyrite developed in bioclastic limestone, LM040, ordinary thin section, stained with alizarin red S, single polarized light; o—bioclastic limestone with brachiopod fossil fragments in the center of the photo, LM042, ordinary thin section, single polarized light; p—bioclastic limestone fragments of brachiopod fossils and foraminifera undergoing selective dolomitization, LM042, ordinary thin section, stained with alizarin red S, single polarized light

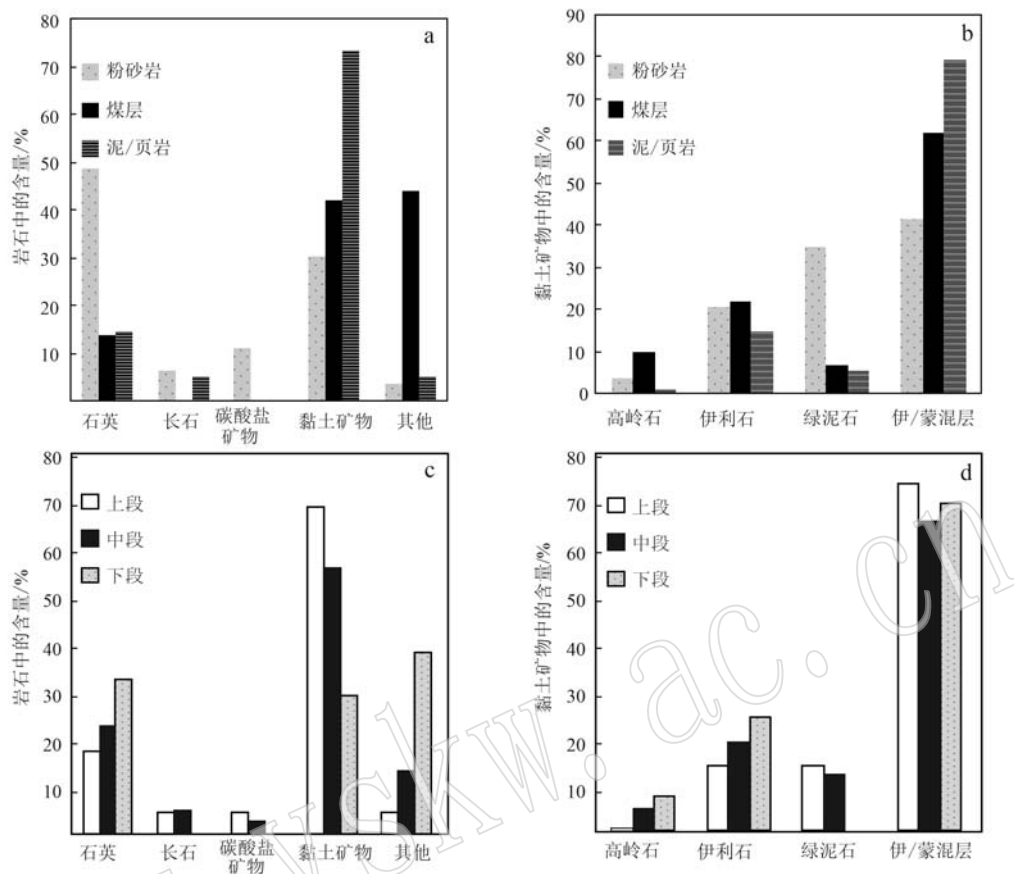


图 6 黔西北大方地区龙峰剖面龙潭组矿物组成直方图

Fig. 6 Histogram of mineral composition of the Longtan Formation in Longfeng profile of Dafang area, Northwest Guizhou

的特点。长石主要分布在龙潭组中段和上段,而碳酸盐矿物中,铁白云石和方解石主要见于龙潭组上段地层中,菱铁矿主要发育于龙潭组中段,个别样品中菱铁矿的含量高达 60%,形成与煤层毗邻的菱铁矿薄层。就具体的黏土矿物组成而言,龙潭组 3 个地层段中均表现为以伊/蒙混层占绝对优势(图 6d),下段、中段与上段伊/蒙混层在黏土矿物中的平均含量大约为 69%、66% 和 73%;其次为伊利石,由下至上平均含量依次为 23.8%、18.7% 和 13.5%;绿泥石主要发育于龙潭组中段和上段地层中,其在黏土矿物中的平均含量分别为 11.9% 和 13.5%;龙潭组上段高岭石仅个别样品中发育,其含量不足 1%,龙潭组中段高岭石主要发育于其下部和上部,其在黏土矿物中的平均含量约为 4.5%,龙潭组下段亦发育高岭石,但由于样品数太少,其平均含量可能不具代表意义。

以往的研究表明,黏土矿物含量与气体吸附能力呈正相关(Ross *et al.*, 2009; Guo *et al.*, 2014)。黏土矿物比石英和碳酸盐岩具有更大的表面积值

(Passey *et al.*, 2010),可以增强气体吸附能力。然而,富含黏土矿物的页岩往往具有延展性,容易变形而不是碎裂,当水力压力和能量注入页岩时,很难成功压裂。同时,脆性矿物含量对基质孔隙度和微裂缝发育、含气量和压裂增产方式有很大影响(李新景等, 2007; 邹才能等, 2010)。脆性矿物含量越高的页岩,其压裂产生裂缝的能力越强,有利于页岩气的开发。因此,泥页岩的矿物成分多样,页岩气含量及其后期压裂效果与页岩的矿物(尤其是脆性矿物和黏土矿物含量)组成息息相关,不同的矿物组成具有不同的物化特征。根据矿物的脆性指数(BRIT)的计算公式(郭旭升, 2014)计算可知,黔西北地区龙潭组泥页岩的脆性指数介于 13%~69% 之间,平均值为 41.3%,脆性指数偏低。目前,一般而言,具备商业开发条件的页岩其脆性矿物含量高于 40%(张鹏, 2015)。相较于已获得商业开发的奥陶系五峰组—志留系龙马溪组地层而言,研究区龙潭组泥页岩中高黏土矿物含量和相对较低的脆性矿物含量及脆性指数增加了压裂难度(图 7a)。但是,黏土矿物中伊

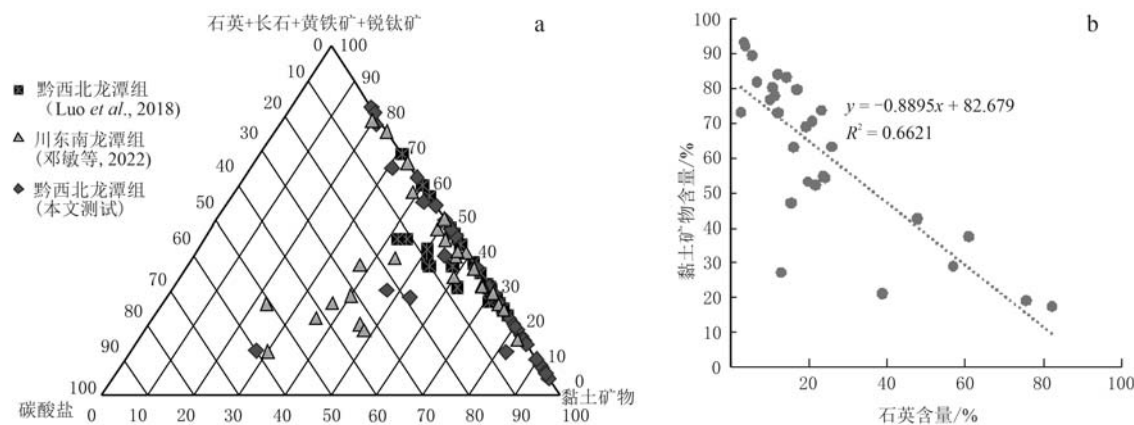


图 7 黔西北及邻区龙潭组中主要矿物三端员分布图(a)和黏土矿物含量与石英含量相关性图(b)

Fig. 7 Ternary diagram of main minerals (a) and correlation diagram between clay mineral and quartz content (b) of the Longtan Formation in Northwest Guizhou and adjacent areas

利石脆性高,伊/蒙混层次之,蒙脱石韧性高,不易断裂,因而大方地区龙潭组地层中高伊利石和伊/蒙混层矿物含量一定程度上可能会改善压裂效果。

## 4 烃源岩的地球化学特征

### 4.1 有机质丰度

#### 4.1.1 总有机碳(TOC)含量

总有机碳(TOC)含量是页岩气形成和富集的物质保障,能较好地反映页岩生烃能力并影响烃类气体的赋存状态及含气性(邓恩德等,2020b)。TOC对页岩的气吸附能力也有决定性的影响,是控制甲烷吸附能力的最重要因素(Ross et al., 2009; He et al., 2019)。TOC含量越高,页岩气的生烃潜力越大,吸附能力越强。目前页岩气商业开采的TOC下限一般为2%。但也有少数学者提出,高成熟阶段页岩TOC下限可以降低到1%(Curtis, 2002; Jarvie et al., 2007; 邹才能等, 2010)。

龙潭组炭质泥(页)岩、粉砂质泥岩样品的残余总有机碳(TOC)含量在0.3%~8.6%之间,平均值为3.2%;煤岩样品的TOC含量在13.5%~60.9%之间,平均值为42.9%;粉砂岩、细-中砂岩样品的TOC含量在1.4%~5.6%之间,平均值为2.2%(表1)。与海相五峰-龙马溪组往往具有自下而上TOC含量降低的趋势不同(兰叶芳等,2021a, 2021b),海陆过渡相岩石样品的有机质丰度受岩性变化的控制明显。由于龙潭组岩性受过渡带沉积环境的影响。岩性垂向变化较为复杂,页岩、煤层、粉砂质页岩、粉砂

岩交替出现。因此,页岩的TOC含量一般表现为高值和低值交替出现(图3)。煤岩样品具有非常高的TOC含量,显示强大的煤层气生烃潜力(图8a)。约有80%的泥页岩样品TOC含量超过2%,说明大部分样品具有较好的页岩气资源潜力。三者相较而言,粉砂岩致密气资源潜力最差。因此,根据龙潭组的纵向岩性组合特征,煤层发育而泥页岩分布频率高的龙潭组中段具有最高的TOC平均含量,约为14.5%,龙潭组下段次之,约为5.6%,龙潭组上段TOC平均含量则不足3%(图8c)。

#### 4.1.2 岩石热解生烃潜量

热解分析是根据有机生油理论及干酪根热降解成烃机制,利用Rock-Eval仪器设备,在还原条件下对样品进行加热降解、裂解并检测其产物的方法,可用于评价烃源岩有机质丰度、类型、成熟度,估算烃源岩生烃潜力,识别储层含油气性。烃源岩热解分析获取的生烃潜量( $S_1+S_2$ )可以用于反映烃源岩有机质丰度,其中, $S_1$ 代表已经有效转化为烃类的原始生烃潜力部分, $S_2$ 代表生烃潜力的剩余部分。生烃潜量低于2 mg/g只具有生成天然气的潜力;2~6 mg/g为中等烃源岩;6 mg/g以上为好烃源岩(蒋有录等,2016)。根据研究区泥页岩样品的热解分析结果(表1),其生烃潜量( $S_1+S_2$ )变化在0.06~0.24 mg/g之间,均小于2 mg/g,也就是说属于中等以下的烃源岩,仅具备生气潜力;煤岩样品生烃潜量为0.9~4.0 mg/g,平均值2.68 mg/g,为中等烃源岩;粉砂岩样品的生烃潜力最差,其生烃潜量平均值

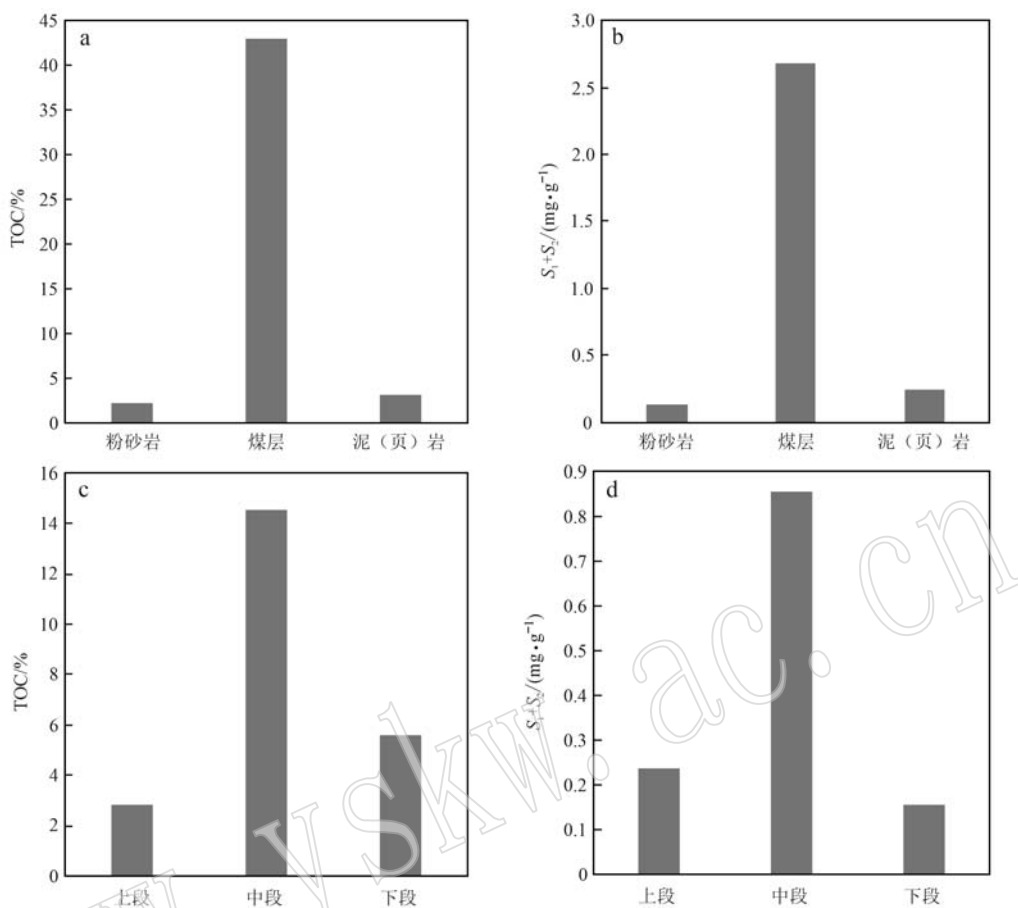


图 8 黔西北大方地区龙潭组不同岩性和层段有机碳(TOC)含量和生烃潜量( $S_1+S_2$ )分布直方图

Fig. 8 Histogram of total organic carbon content (TOC) and hydrocarbon generation potential ( $S_1+S_2$ ) in different lithologies and intervals of the Longtan Formation in the Dafang area of Northwest Guizhou

为 0.13 mg/g(图 8b)。不同岩石类型的岩石热解结果所揭示的生烃潜力与 TOC 分析结果是一致的(图 8a、8b), 纵向不同岩性组合段的变化特征也体现出相似的特征(图 8c、8d)。因此, 从有机质丰度来看, 龙潭组中段是该地层中最具勘探潜力的层段。

#### 4.2 有机质类型

烃源岩中有机质的类型是其质量指标, 也是评价烃源岩生烃能力的重要参数, 不同类型的有机质具有不同的生油气潜力, 会形成不同的产物。一般根据干酪根的类型将其划分为 I 型、II 型和 III 型。通过干酪根的显微组分分析, 研究区龙潭组泥页岩的干酪根主要由壳质组、镜质组和惰质组组成, 尤其以壳质组和镜质组占主导, 未发现腐泥组的显微组分(图 9、图 10a)。通过类型指数的计算, 龙潭组有机质类型为 II<sub>2</sub>-III 型干酪根(表 1), 虽然部分泥页岩样品中 II<sub>2</sub> 型干酪根发育, 但是总体以 III 型干酪根为

主, 表明其有机质主要来源于高等植物, 生油潜力小, 以生气为主。

根据岩石的热解分析, 氢指数 ( $S_2/TOC$ , 简称 HI) 大多小于 10, 也表明其原始氢含量低, 属于典型的 III型干酪根特征(表 1)。不同类型的干酪根具有不同的生烃潜力和不同的产物, 这与有机质的组成和结构有关(Pu et al., 2015)。显微组分类型和组成的差异是导致不同类型干酪根具有不同生烃阈值的关键原因。腐殖型干酪根(III型)比腐泥型干酪根(I型)更早进入生气窗口(图 10b)。I型和 II型(高 HI)干酪根比 II/III型和 III型(低 HI)具有更大的甲烷吸附能力。但对于单位体积的 TOC, III型可以比 I型和 II型吸附更多的甲烷, 这可能与 III型干酪根中较高的孔隙体积有关(Chalmers et al., 2008)。因此, 从这个角度来讲, 龙潭组 III型干酪根的发育意味着相对较早进入生气窗口并具有一定的

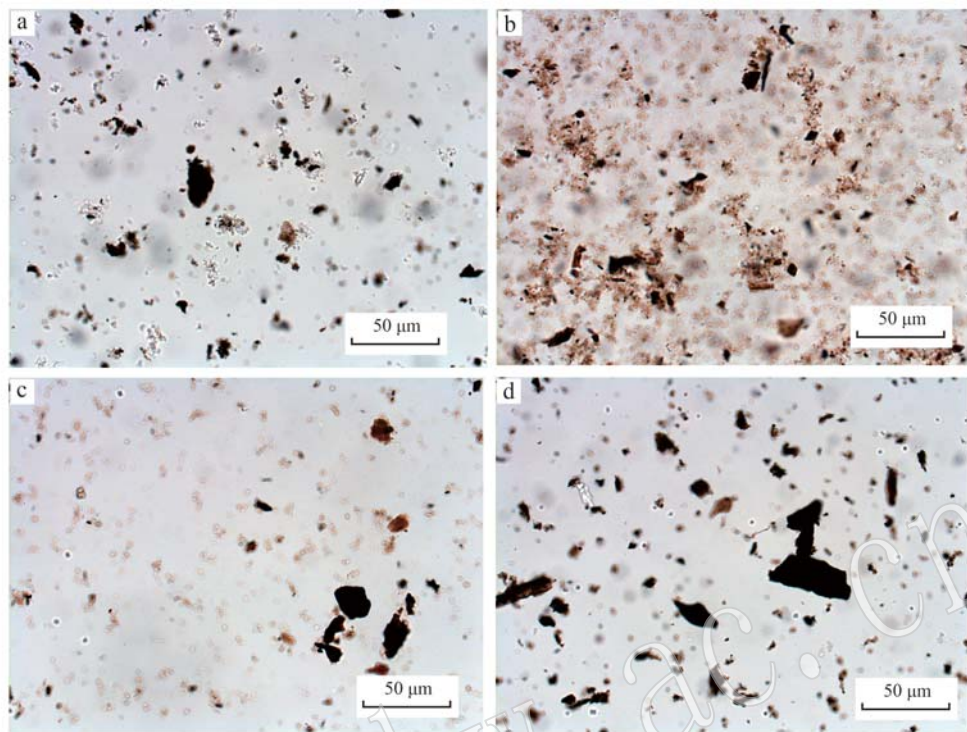


图9 黔西北大方地区龙潭组干酪根显微组分照片

Fig. 9 Microphotos of the macerals of kerogen from the Longtan Formation in the Dafang area of Northwest Guizhou

a—干酪根显微组分以壳质组(无定形体)和惰质组(丝质体)为主,同时发育镜质组(结构镜质体); b—以发育壳质组的无定形体占主导,其次为结构和无结构镜质体以及由高等植物木质部分经强烈碳化而成的丝质体; c—照片中以镜质体和壳质组(无定形体)占主导,见少量丝质体发育; d—照片中见大量丝质体发育,少量褐色无定形体和透明—半透明镜质体

a—the macerals of kerogen are mainly composed of chitin (amorphous) and inertinite (filamentous), while vitrinite (structural vitrinite) is also developed; b—the amorphous forms dominated by the development of chitin, followed by structural and unstructured vitrinite, as well as filamentous bodies formed by strong carbonization of higher plant woody parts; c—vitrinite and chitin (amorphous) are dominant, with a small amount of inertinite; d—a large number of filamentous bodies are developed, with a small amount of brown amorphous bodies and transparent-semi transparent vitrinite bodies

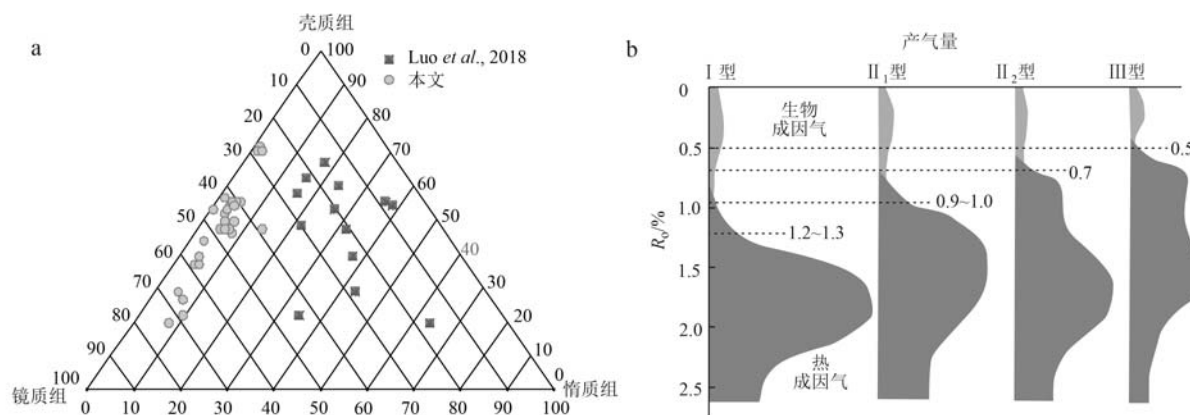


图10 黔西北龙潭组干酪根镜检结果三角投点图(a)和不同类型干酪根产气量图(b, 据 Pu et al. , 2015)

Fig. 10 Triangle plot of kerogen composition (a) and gas production of different types of kerogen (b, Pu et al. , 2015) in the Longtan Formation, Northwest Guizhou

表1 黔西北大方地区龙峰剖面龙潭组干酪根显微组分、镜质体反射率、有机碳含量和岩石热解分析结果

Table 1 Kerogen macerals, vitrinite reflectance, organic carbon content and rock pyrolysis data of the Longtan

Formation samples in the Longfeng profile of Dafang area, Northwest Guizhou

样号	岩石类型	壳质组/%	镜质组/%	惰质组/%	TI	干酪根类型	$R_o$ /%	$S_0'$ (mg · g <sup>-1</sup> )	$S_1'$ (mg · g <sup>-1</sup> )	$S_2'$ (mg · g <sup>-1</sup> )	$S_1+S_2'$ (mg · g <sup>-1</sup> )	TOC/%	HI	PI	$t_{max}$ /°C
LM003	粉砂岩	38	56	6	-29	III	2.95	0.0037	0.0149	0.1406	0.1555	5.56	2.53	0.10	586
LM004	粉砂岩											2.22			
LM005	泥(页)岩	34	59	7	-34.3	III	2.80	0.0038	0.0119	0.0783	0.0902	2.00	3.92	0.13	586
LM006	粉砂岩	32	61	7	-36.8	III	2.42	0.0037	0.0213	0.0499	0.0712	1.90	2.63	0.30	528
LM007	泥(页)岩							0.0036	0.0194	0.0560	0.0754	1.07	5.23	0.26	513
LM008	泥(页)岩	62	32	6	1	II <sub>2</sub>	1.11	0.0035	0.0105	0.0376	0.0481	0.54	6.94	0.22	522
LM010	煤层	17	74	9	-56	III	2.26					39.40			
LM011	煤层	19	70	11	-54	III	2.92	0.0077	0.0468	3.9356	3.9824		0.01	587	
LM011-1	煤层	23	68	9	-48.5	III	2.99	0.0047	0.0376	3.6429	3.6805	54.80	6.65	0.01	588
LM012	粉砂岩							0.0052	0.0128	0.1473	0.1601	1.69	8.72	0.08	587
LM013	泥(页)岩	69	27	4	10.3	II <sub>2</sub>	1.22	0.0036	0.0080	0.0544	0.0624		0.13	546	
LM014	泥(页)岩	41	49	10	-26.3	III	2.65	0.0037	0.0148	0.4616	0.4764	4.86	9.50	0.03	587
LM015	煤层	25	68	7	-45.5	III	2.70					60.90			
LM016	泥(页)岩	48	43	9	-17.3	III	2.62	0.0036	0.0300	0.7252	0.7552	8.56	8.47	0.04	587
LM017	泥(页)岩	43	47	10	-23.8	III	2.50	0.0046	0.0148	0.3752	0.3900	5.19	7.23	0.04	588
LM020	粉砂岩							0.0036	0.0155	0.0520	0.0675	0.83	6.30	0.23	582
LM021	泥(页)岩	41	51	8	-25.8	III	2.85	0.0037	0.0245	0.1574	0.1819	2.43	6.48	0.13	583
LM022	泥(页)岩	61	33	6	-0.3	III	2.92	0.0036	0.0167	0.1644	0.1811	2.97	5.54	0.09	583
LM023	煤层											48.60			
LM024	煤层	41	49	10	-26.3	III	2.70	0.0044	0.0251	0.8922	0.9173	13.50	6.61	0.03	583
LM025	泥(页)岩	46	50	4	-18.5	III	1.30	0.0036	0.0250	0.2040	0.2290	2.78	7.34	0.11	584
LM026	泥(页)岩	47	46	7	-18	III	2.66	0.0039	0.0404	0.3415	0.3819	4.64	7.36	0.11	584
LM027	煤层	48	44	8	-17	III	2.90	0.0042	0.0257	2.8521	2.8778		0.01	584	
LM028	煤层	41	42	17	-28	III	2.88	0.0043	0.0223	1.8993	1.9216	31.00	6.13	0.01	583
LM029	泥(页)岩	71	25	4	12.8	II <sub>2</sub>	1.02	0.0079	0.0289	0.1081	0.1370	1.85	5.84	0.21	586
LM030	煤层	48	45	7	-16.8	III	2.72	0.0052	0.0507	2.6398	2.6905	52.20	5.06	0.02	585
LM031	泥(页)岩	32	60	8	-37	III	2.02	0.0040	0.0173	0.1477	0.1650	3.09	4.78	0.10	586
LM032	粉砂岩	45	48	7	-20.5	III	2.98	0.0035	0.0153	0.1354	0.1507	1.42	9.54	0.10	584
LM033	泥(页)岩	72	25	3	14.3	II <sub>2</sub>	1.16	0.0036	0.0091	0.0448	0.0539	0.30	14.74	0.17	507
LM034	泥(页)岩	83	15	2	28.3	II <sub>2</sub>	1.19	0.0034	0.0194	0.0404	0.0598	0.41	9.85	0.32	512
LM035	泥(页)岩	70	26	4	11.5	II <sub>2</sub>	1.30	0.0037	0.0134	0.3633	0.3767	3.24	11.21	0.04	472
LM036	泥(页)岩	43	49	8	-23.3	III	2.66	0.0050	0.0157	0.3577	0.3734	4.35	8.22	0.04	586
LM037	泥(页)岩	46	47	7	-19.3	III	2.89	0.0051	0.0129	0.1279	0.1408	1.71	7.48	0.09	593
LM038	泥(页)岩	41	50	9	-26	III	2.95	0.0050	0.0141	0.1253	0.1394	1.81	6.92	0.10	589
LM039	泥(页)岩	61	32	7	-0.5	III	1.11	0.0038	0.0254	0.3924	0.4178	7.52	5.22	0.06	589
LM041	泥(页)岩	47	45	8	-18.3	III	2.52	0.0040	0.0191	0.3456	0.3647	3.88	8.91	0.05	587
LM043	粉砂岩	49	46	5	-15	III	2.68	0.0038	0.0369	0.1582	0.1951	2.13	7.43	0.19	588

TI—干酪根的类型指数;  $R_o$ —镜质体反射率;  $S_0'$ —岩石中轻烃(C1~C7)含量;  $S_1'$ —岩石中残留烃含量(测  $S_0'$ 时, 不包括 C1~C7 烃);  $S_2'$ —岩石中裂解烃含量;  $S_3$ —岩石热解生成的 CO<sub>2</sub>量, 代表岩石样品在 600°C 下不能裂解的残余有机碳, 代表部分胶质和沥青质; HI—氢指数; PI—产率指数; TOC—总有机碳含量;  $t_{max}$ — $S_2'$ 峰值最高温度。

### 甲烷吸附能力。

#### 4.3 有机质成熟度

已有的勘探开发及研究认为, 烃源岩中有机质的热演化程度(即有机质成熟度)是评价生气和产能的关键地球化学参数(Jarvie *et al.*, 2007)。有机质成熟度不仅影响产气潜力, 还影响气体吸附能力(聂海宽等, 2009)。随着热成熟度的增加, 生气潜力降低, 但气体吸附能力增加。此次研究中, 粉砂岩样品的镜质体反射率( $R_o$ )为 2.42%~2.98% (平均值 2.76%), 煤岩样品  $R_o$  值为 2.26%~2.99% (平均值 2.76%), 而泥(页)岩样品相应  $R_o$  值为 1.02%~2.99% (平均值 2.07%), 其中大约有 25% 的样品  $R_o$  值介于 1.0%~1.3% 之间, 其余 75% 左右的样品  $R_o$

值均大于 2%。纵向上, 自龙潭组下段至龙潭组上段镜质体反射率呈现逐渐增加的趋势, 下、中和上段的  $R_o$  平均值依次为 2.05%、2.42% 和 2.95%。鉴于不同干酪根的热演化差异, I 型和 II<sub>1</sub> 型干酪根的  $R_o$  下限为 1.1%, II<sub>2</sub> 型和 III 型干酪根的  $R_o$  下限为 0.9% (图 10b)。龙潭组干酪根为 II<sub>2</sub> 型和 III 型, 高  $R_o$  值表明龙潭组烃源岩大部分为高-过成熟阶段, 热演化处于干气窗口(Luo *et al.*, 2018), 龙潭组下段和中段具有更强的生气潜力, 龙潭组上段生气潜力较弱。根据岩石热解获得的数据, 龙潭组样品的峰温  $t_{max}$  值在 472~593°C 之间(表 1), 大部分样品的  $t_{max}$  值大于 500°C, 属于高-过成熟演化阶段, 这与镜质体反射率的研究结果是一致的。有机质成熟度的

高低决定着经埋藏后是否能达到生气窗。前人研究认为,  $t_{max} > 470^{\circ}\text{C}$  标志着生气窗口的开始, 相应地龙潭组此次研究测试的样品均落在生气窗内(图 11)。根据总生烃潜力( $S_1 + S_2$ )与残余有机碳总量 TOC 的相关性图表明, 由于相对较高的成熟度, 龙潭组泥页

岩目前的生烃潜力较低, 仅具有生气潜力(图 12)。然而, 龙潭组泥页岩的高成熟度( $R_o$ )和高剩余有机碳总量(TOC)则表明, 龙潭组依然具有一定的产气潜能(图 11、图 12)。

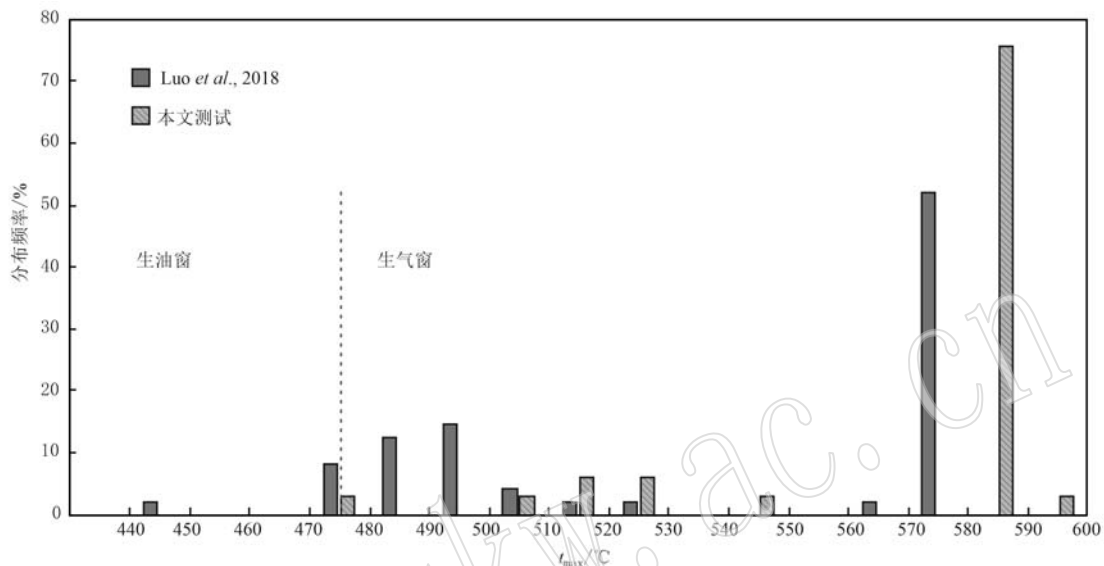


图 11 黔西北大方地区龙潭组峰温  $t_{max}$  分布直方图

Fig. 11 Histograms of the  $t_{max}$  in the Longtan Formation of Dafang area, Northwest Guizhou

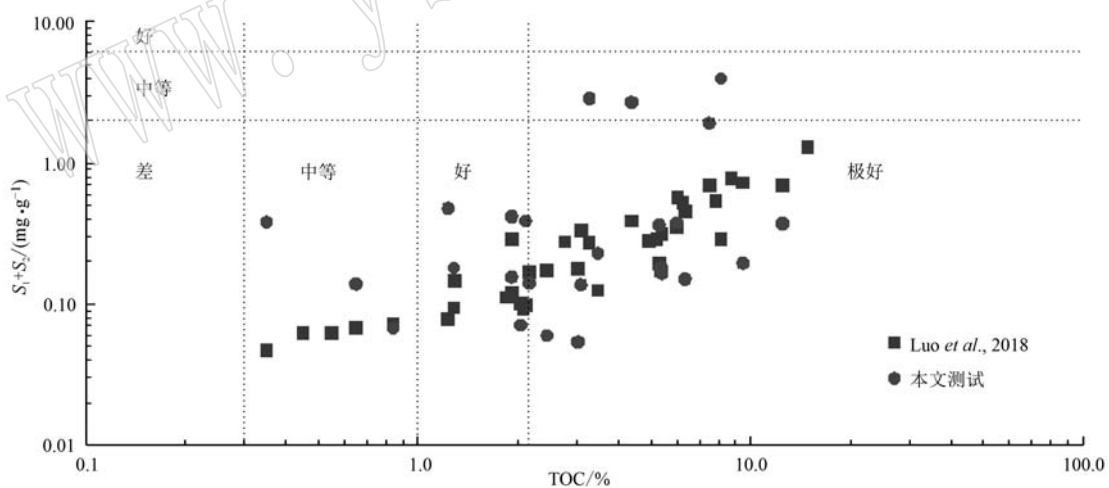


图 12 黔西北大方地区龙潭组泥页岩生烃潜量( $S_1 + S_2$ )与 TOC 含量交会图

Fig. 12 Total hydrocarbon generation potential ( $S_1 + S_2$ ) versus TOC plot of shales in the Longtan Formation of Dafang area, Northwest Guizhou

## 5 结论

通过黔西北大方地区龙潭组野外剖面勘测和室内综合分析, 主要得出以下几点结论:

(1) 黔西北大方地区海陆过渡相龙潭组泥页

岩、煤层和粉砂岩交替发育, 龙潭组下段以深灰色-灰黑色薄层泥岩为主, 中段以薄层砂泥岩互层与煤层交替发育为主体特征, 上段普遍发育极薄层泥岩夹粉砂岩和灰岩层。煤层主要发育于中段和下段, 泥页岩单层厚度变化较大, 总厚度大约为 80 m 左右。

(2) 大方地区龙潭组整体矿物组成上具有高黏

土矿物(伊/蒙混层为主)含量和低脆性指数特征,龙潭组下段、中段至上段,黏土矿物含量升高,石英等脆性矿物含量降低,相应吸附能力增强的同时也会增加压裂开发的难度。

(3) 大方地区龙潭组有机质以Ⅲ型干酪根为主,少量Ⅱ<sub>2</sub>型干酪根,热演化程度高,处于生气气阶段,自下而上,热演化程度逐渐增加,生气能力逐渐减弱。结合有机质丰度分析,龙潭组地层中,煤层生烃潜力最强,泥页岩次之,粉砂岩最弱。3个层段中,龙潭组中段具有最高的TOC含量和生烃潜量。综合研究表明,龙潭组中段是大方地区非常规气勘探开发的较有利目标层段。

## References

- Cao Lei and Guo Yinghai. 2020. Pore structure and fractal characteristics of mud shale in Shanxi Formation of Wuxiang block[J]. *Acta Petrologica et Mineralogica*, 39(3): 283~290 (in Chinese with English abstract).
- Chalmers G R L and Bustin R M. 2008. Lower cretaceous gas shales in northeastern British Columbia, part I: Geological controls on methane sorption capacity[J]. *Bulletin of Canadian Petroleum Geology*, 56(1): 1~21.
- Curtis J B. 2002. Fractured shale-gas systems[J]. *AAPG Bulletin*, 86(11): 1921~1938.
- Deng Ende, Yan Zhihua, Jiang Bingren, et al. 2020a. Reservoir characteristics of marine-continental shale gas in Upper Permian Longtan Formation, western Guizhou Province[J]. *Petroleum Exploration and Development*, 42(3): 467~476 (in Chinese with English abstract).
- Deng Ende, Yi Tongsheng, Yan Zhihua, et al. 2020b. Accumulation condition and shale gas potential of the marine-terrestrial transitional facies: A case study of Jinshacan 1 well of Longtan Formation in northern Guizhou[J]. *Journal of China University of Mining & Technology*, 49(6): 1166~1181 (in Chinese with English abstract).
- Deng Min, Lan Yefang, Cheng Jinxiang, et al. 2022. Shale gas (CBM) potential of Longtan Formation in Shibao mining area, Southeast Sichuan: A case study of Well SD1[J]. *Acta Geoscientica Sinica*, 43(3): 295~308 (in Chinese with English abstract).
- Dong Dazhong, Qiu Zheng, Zhang Leifu, et al. 2021. Progress on sedimentology of transitional facies shales and new discoveries of shale gas [J]. *Acta Sedimentologica Sinica*, 39(1): 29~45 (in Chinese with English abstract).
- Dong Dazhong, Wang Yuman, Li Xinjing, et al. 2016. Breakthrough and prospect of shale gas exploration and development in China[J]. *Natural Gas Industry*, 36(1): 19~32 (in Chinese with English abstract).
- Feng Dongjun. 2023. Sweet spot assessment and its significance for the marine-continental transitional shale gas of Permian Longtan Fm. in southeastern Sichuan Basin[J]. *Oil & Gas Geology*, 37(6): 641~653 (in Chinese with English abstract).
- Guo H J, Jia W L, Peng P A, et al. 2014. The composition and its impact on the methane sorption of lacustrine shales from the Upper Triassic Yanchang Formation, Ordos Basin, China[J]. *Marine Petrology Geology*, 57(2): 509~520.
- Guo Wei, Gao Jinliang, Li Hai, et al. 2023. The geological and production characteristics of marine-continental transitional shale gas in China: Taking the example of shale gas from Sanxi Formation in Ordos Basin and Longtan Formation in Sichuan Basin[J]. *Mineral Exploration*, 14(3): 448~458 (in Chinese with English abstract).
- Guo Xusheng. 2014. Enrichment Mechanism and Exploration Technology of Jiaoshiba Block in Fuling Shale Gas Field[M]. Beijing: Science Press (in Chinese).
- Guo Xusheng, Hu Dongfeng, Liu Ruobing, et al. 2018. Geological conditions and exploration potential of Permian marine-continent transitional facies shale gas in the Sichuan Basin[J]. *Natural Gas Industry*, 38(10): 11~18 (in Chinese with English abstract).
- He Guisong, He Xipeng, Gao Yuqiao, et al. 2023. Discovery of shale gas of Permian Longtan Formation in Nanchuan area, southeast Sichuan Basin[J]. *Geology in China*, 50(3): 965~966 (in Chinese).
- He Q, Dong T, He S, et al. 2019. Methane adsorption capacity of marine-continental transitional facies shales: The case study of the Upper Permian Longtan Formation, northern Guizhou Province, Southwest China [J]. *Journal of Petroleum Science and Engineering*, 183: 1~15.
- Hu Haiyang, Bai Lina, Zhao Lingyun, et al. 2019. Drainage and mining control study on co-mining Coal Measure Gas of Longtan Formation in Western Guizhou Region[J]. *Safety in Coal Mines*, 50(1): 175~178 (in Chinese with English abstract).
- Jarvie D M, Hill R J, Ruble T E, et al. 2007. Unconventional shale-gas systems: The Mississippian Barnett Shale of north-central Texas as one model for thermogenic shale-gas assessment[J]. *AAPG Bulletin*, 91(4): 475~499.
- Jia Lilong, Shu Jiansheng, Jiang Zaibing, et al. 2021. Study on formation conditions and reservoir characteristics of marine-terrigenous facies coal measures shale gas in western Guizhou[J]. *Coal Science and Technology*, 49(10): 201~207 (in Chinese with English abstract).
- Jiang Youlu and Zha Ming. 2016. *Petroleum Geology and Exploration* [M]. Beijing: Petroleum Industry Press (in Chinese).
- Jiao Fangzheng, Wen Shengming, Liu Xiangjun, et al. 2023. Research progress in exploration theory and technology of transitional shale gas in the Ordos Basin[J]. *Natural Gas Industry*, 43(4): 11~23 (in Chinese with English abstract).

- Chinese with English abstract).
- Kuang Lichun, Dong Dazhong, He Wenyuan, et al. 2020. Geological characteristics and development potential of transitional shale gas in the east margin of the Ordos Basin, NW China [J]. Petroleum Exploration and Development, 47(3): 435~446 (in Chinese with English abstract).
- Lan Yefang, Ren Chuanjian, Huang Yu, et al. 2021a. The evaluation of shale gas source rocks in Upper Ordovician Wufeng Formation-Lower Silurian Longmaxi Formation of Yanzikou area, northwest Guizhou [J]. Acta Petrologica et Mineralogica, 40(1): 49~64 (in Chinese with English abstract).
- Lan Yefang, Wu Haizhi, Ren Chuanjian, et al. 2021b. Shale reservoir characteristics of Wufeng-Longmaxi Formation in Yanzikou area, northwestern Guizhou [J]. Petroleum Geology and Recovery Efficiency, 28(1): 115~124 (in Chinese with English abstract).
- Li Jian, Wang Xiaobo, Hou Lianhua, et al. 2021. Geochemical characteristics and resource potential of shale gas in Sichuan Basin [J]. Natural Gas Geoscience, 32(8): 1093~1106 (in Chinese with English abstract).
- Li Juan, Yu Bingsong, Xia Xianghua, et al. 2015. The characteristics of the Upper Permian shale reservoir in the northwest of Guizhou Province, China [J]. Earth Science Frontiers, 22(1): 301~311 (in Chinese with English abstract).
- Li Xinjing, Hu Suyun and Cheng Keming. 2007. Suggestions from the development of fractured shale gas in North America [J]. Petroleum Exploration and Development, 34(4): 392~400 (in Chinese with English abstract).
- Liu Zengqin. 2020. Reservoir Characterization of the Marine-continental Transitional Tight Sandstones in the Longtan Fomation, West Guizhou, China [D]. China University of Geosciences (Beijing) (in Chinese with English abstract).
- Luo W, Hou M C, Liu X C, et al. 2018. Geological and geochemical characteristics of marine-continental transitional shale from the Upper Permian Longtan formation, Northwestern Guizhou, China [J]. Marine and Petroleum Geology, 89: 58~67.
- Ma Xiao. 2021. Fine Characterization of Shale Reservoir of Longtan Formation in Western Guizhou [D]. China University of Geosciences (Beijing) (in Chinese with English abstract).
- Nie Haikuan, He Faqi and Bao Shujing. 2011. Peculiar geological characteristics of shale gas in China and its exploration counter measures [J]. Natural Gas Industry, 31(11): 111~116 (in Chinese with English abstract).
- Nie Haikuan, Tang Xuan and Bian Ruikang. 2009. Controlling factors for shale gas accumulation and prediction of potential development area in shale gas reservoir of South China [J]. Acta Petrolei Sinica, 30(4): 484~491 (in Chinese with English abstract).
- Passey Q R, Bohacs K M, Esch W L, et al. 2010. From oil-prone source rock to gas-producing shale reservoir-geologic and petrophysical characterization of unconventional shale-gas reservoirs. SPE-131350 [C]//CPS/SPE International Oil & Gas Conference and Exhibition in China. June 8~10, Beijing, China.
- Pu B L, Dong D Z, Zhao J Z, et al. 2015. Differences between marine and terrestrial shale gas accumulation: Taking Longmaxi Shale Sichuan Basin and Yanchang Shale Ordos Basin as example [J]. Acta Geologica Sinica (English Edition), 89(supp. ): 200~206.
- Ross D J K and Bustin R M. 2009. The importance of shale composition and pore structure upon gas storage potential of shale gas reservoirs [J]. Marine Petrology Geology, 26(6): 916~927.
- Sun Quanhong. 2014. Forming Condition and Distribution Prediction of Shale Gas of Longtan Formation in Northwest Guizhou [D]. China University of Geosciences (Beijing) (in Chinese with English abstract).
- Sun Wenjinbin. 2021. Pore Structure and Evolution Characteristics of the Cambrian Niutitang Formation in Northern Guizhou [D]. Guizhou University (in Chinese with English abstract).
- Wang Shengjian, Gao Wei, Guo Tianxu, et al. 2020. The discovery of shale gas, coalbed gas and tight sandstone gas in Permian Longtan Formation, northern Guizhou Province [J]. Geology in China, 47(1): 249~250 (in Chinese).
- Wang Xiaolei, Cao Zhengjie, Yang Qiangqiang, et al. 2020. Geological conditions of shale gas formation in Longtan Formation in Eastern Sichuan Region and evaluation of promising areas [J]. Science Technology and Engineering, 20(20): 8139~8145 (in Chinese with English abstract).
- Wei Xiaoliang. 2020. Pore Effectiveness of Marine and Continental Transitional Shale and Its Effect on Shale Gas Diffusion: A Case Study of Permian Shale in Southern North China Basin [D]. China University of Geosciences (Beijing) (in Chinese with English abstract).
- Yuan Yuyang, Liu Yonglin and Wang Ying. 2020. "Sweet spot" effect and mechanism of shale fracture development in Longmaxi Formation, northwestern Guizhou [J]. Acta Petrologica et Mineralogica, 39(6): 808~818 (in Chinese with English abstract).
- Zhai Gangyi, Wang Yufang, Liu Guoheng, et al. 2020. Enrichment and accumulation characteristics and prospect analysis of the Permian marine continental multiphase shale gas in China [J]. Sedimentary Geology and Tethyan Geology, 40(3): 102~117 (in Chinese with English abstract).
- Zhang Jinchuan, Shi Miao, Wang Dongsheng, et al. 2021. Fields and directions for shale gas exploration in China [J]. Natural Gas Industry, 41(8): 69~80 (in Chinese with English abstract).
- Zhang Peng. 2015. The Control Mechanism and Application of Sedimentary Environment for the Shale Gas Accumulation [D]. China Univer-

- sity of Geosciences (Beijing) (in Chinese with English abstract).
- Zou Caineng, Dong Dazhong, Wang Shejiao, et al. 2010. Geological characteristics formation mechanism and resource potential of shale gas in China [J]. Petroleum Exploration and Development, 37(6): 641~653 (in Chinese with English abstract).
- Zou C, Yang Z, Sun S, et al. 2020. "Exploring petroleum inside source kitchen": Shale oil and gas in Sichuan Basin [J]. Science China Earth Sciences, 63: 934~953.
- ### 附中文参考文献
- 曹磊, 郭英海. 2020. 武乡区块山西组泥页岩孔隙结构及分形特征研究 [J]. 岩石矿物学杂志, 39(3): 283~290.
- 邓恩德, 颜智华, 姜秉仁, 等. 2020a. 黔西地区上二叠统龙潭组海陆交互相页岩气储层特征 [J]. 石油实验地质, 42(3): 467~476.
- 邓恩德, 易同生, 颜智华, 等. 2020b. 海陆过渡相页岩气聚集条件及勘探潜力研究: 以黔北地区金沙参1井龙潭组为例 [J]. 中国矿业大学学报, 49(6): 1166~1181.
- 邓敏, 兰叶芳, 程锦翔, 等. 2022. 川东南石宝矿区龙潭组页岩气(煤层气)潜力分析——以SD1井为例 [J]. 地球学报, 43(3): 295~308.
- 董大忠, 王玉满, 李新景, 等. 2016. 中国页岩气勘探开发新突破及发展前景思考 [J]. 天然气工业, 36(1): 19~32.
- 董大忠, 邱振, 张磊夫, 等. 2021. 海陆过渡相页岩气层系沉积研究进展与页岩气新发现 [J]. 沉积学报, 39(1): 29~45.
- 冯动军. 2023. 川东南二叠系龙潭组海-陆过渡相页岩气甜点评价及意义 [J]. 石油与天然气地质, 44(3): 778~788.
- 郭为, 高金亮, 李海, 等. 2023. 中国海陆过渡相页岩气地质开发特征——以鄂尔多斯盆地东缘山西组和四川盆地龙潭组页岩气为例 [J]. 矿产勘察, 14(3): 448~458.
- 郭旭升. 2014. 涪陵页岩气田焦石坝区块富集机理与勘探技术 [M]. 北京: 科学出版社.
- 郭旭升, 胡东风, 刘若冰, 等. 2018. 四川盆地二叠系海陆过渡相页岩气地质条件及勘探潜力 [J]. 天然气工业, 38(10): 11~18.
- 何贵松, 何希鹏, 高玉巧, 等. 2023. 四川盆地东南部南川地区发现二叠系龙潭组页岩气 [J]. 中国地质, 50(3): 965~966.
- 胡海洋, 白利娜, 赵凌云, 等. 2019. 黔西地区龙潭组煤系气共采排采控制研究 [J]. 煤矿安全, 50(1): 175~178.
- 贾立龙, 舒建生, 姜在炳, 等. 2021. 黔西海陆过渡相煤系页岩气成藏条件及储层特征研究 [J]. 煤炭科学技术, 49(10): 201~207.
- 蒋有录, 查明. 2016. 石油天然气地质与勘探 [M]. 北京: 石油工业出版社.
- 焦方正, 温声明, 刘向君, 等. 2023. 鄂尔多斯盆地海陆过渡相页岩气勘探理论与技术研究新进展 [J]. 天然气工业, 43(4): 11~23.
- 匡立春, 董大忠, 何文渊, 等. 2020. 鄂尔多斯盆地东缘海陆过渡相页岩气地质特征及勘探开发前景 [J]. 石油勘探与开发, 47(3): 435~446.
- 兰叶芳, 任传建, 黄喻, 等. 2021a. 黔西北燕子口地区五峰-龙马溪组页岩气源岩评价 [J]. 岩石矿物学杂志, 40(1): 49~64.
- 兰叶芳, 吴海枝, 任传建, 等. 2021b. 黔西北燕子口地区五峰组-龙马溪组泥页岩储层特征 [J]. 油气地质与采收率, 28(1): 115~124.
- 李剑, 王晓波, 侯连华, 等. 2021. 四川盆地页岩气地球化学特征及资源潜力 [J]. 天然气地球科学, 32(8): 1093~1106.
- 李娟, 于炳松, 夏响华, 等. 2015. 黔西北地区上二叠统龙潭组泥页岩储层特征 [J]. 地学前缘, 22(1): 301~311.
- 李新景, 胡素云, 程克明. 2007. 北美裂缝性页岩气勘探开发的启示 [J]. 石油勘探与开发, 34(4): 392~400.
- 刘曾勤. 2020. 黔西地区龙潭组致密砂岩储层评价 [D]. 中国地质大学(北京).
- 马啸. 2021. 黔西地区龙潭组泥页岩储层精细表征 [D]. 中国地质大学(北京).
- 聂海宽, 何发岐, 包书景. 2011. 中国页岩气地质特殊性及其勘探对策 [J]. 天然气工业, 31(11): 111~116.
- 聂海宽, 唐玄, 边瑞康. 2009. 页岩气成藏控制因素及中国南方页岩气发育有利区预测 [J]. 石油学报, 30(4): 484~491.
- 孙全宏. 2014. 黔西北地区龙潭组页岩气形成条件与分布预测 [D]. 中国地质大学(北京).
- 孙文吉斌. 2021. 黔北寒武系牛蹄塘组页岩孔隙结构特征及其演化研究 [D]. 贵州大学.
- 王胜建, 高为, 郭天旭, 等. 2020. 黔北金沙地区二叠系龙潭组取得页岩气、煤层气和致密砂岩气协同发现 [J]. 中国地质, 47(1): 249~250.
- 王晓蕾, 曹正杰, 杨强强, 等. 2020. 川东地区龙潭组页岩气成藏地质条件与有利区评价 [J]. 科学技术与工程, 20(20): 8139~8145.
- 魏晓亮. 2020. 海陆过渡相页岩孔隙有效性及其对页岩气扩散的影响——以南华北盆地二叠系页岩为例 [D]. 中国地质大学(北京).
- 袁余洋, 刘永林, 王瑛. 2020. 黔西北地区龙马溪组页岩有机质和脆性矿物的控缝机制 [J]. 岩石矿物学杂志, 39(6): 808~818.
- 翟刚毅, 王玉芳, 刘国恒, 等. 2020. 中国二叠系海陆交互页岩气富集成藏特征及前景分析 [J]. 沉积与特提斯地质, 40(3): 102~117.
- 张金川, 史森, 王东升, 等. 2021. 中国页岩气勘探领域和发展方向 [J]. 天然气工业, 41(8): 69~80.
- 张鹏. 2015. 沉积环境对页岩气发育的控制作用及应用 [D]. 北京: 中国地质大学(北京).
- 邹才能, 董大忠, 王社教, 等. 2010. 中国页岩气形成机理、地质特征及资源潜力 [J]. 石油勘探与开发, 37(6): 641~653.
- 邹才能, 杨智, 孙莎莎, 等. 2020. “进源找油”: 论四川盆地页岩油气 [J]. 中国科学: 地球科学, 50(7): 903~920.